Publication Year	2021
Acceptance in OA@INAF	2023-02-01T13:15:07Z
Title	Coating samples for the BEaTriX mirrors: surface roughness analysis
Authors	SPIGA, Daniele
Handle	http://hdl.handle.net/20.500.12386/33098
Number	INAF-OAB internal report 2021/01

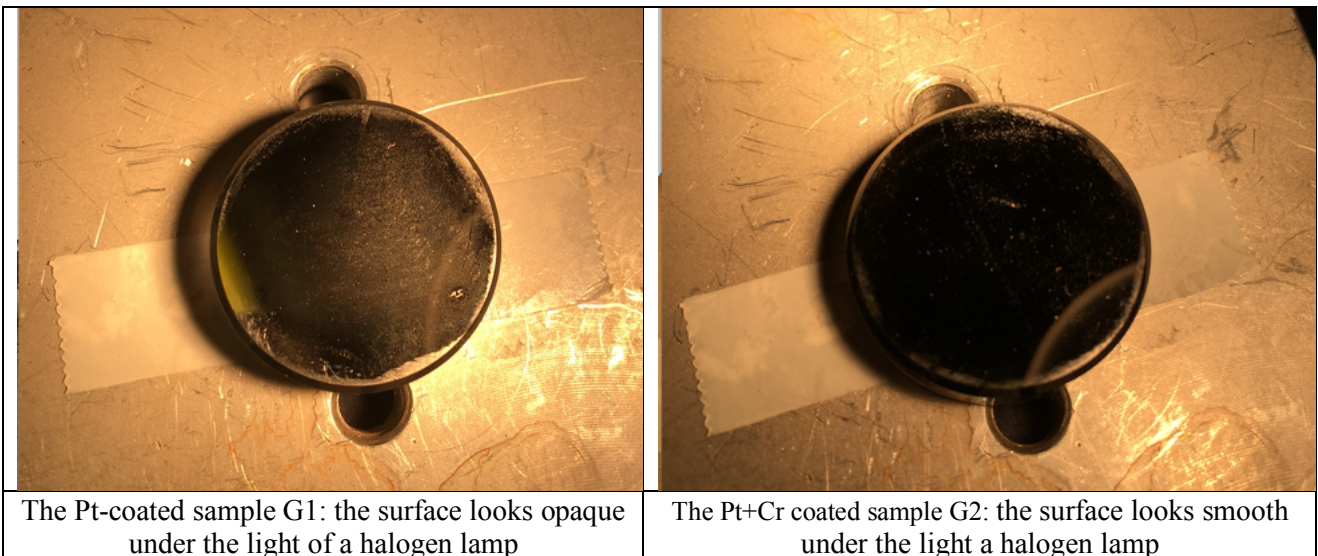*Advanced Telescope for High-Energy Astrophysics* (*ATHENA*)

BEaTriX, the Beam Expander Testing X-ray facility

Coating samples for the BEaTriX mirrors: surface roughness analysis

Technical note by **D. Spiga**, *reviewed by* **B. Salmaso**, *MFT measurements by* **G. Vecchi**

INAF-OAB internal report 01/2021

The Pt-coated sample G1: the surface looks opaque under the light of a halogen lamp	The Pt+Cr coated sample G2: the surface looks smooth under the light a halogen lamp

Contents

Applicable documents

[AD1]. Nis C. Gellert, Sonny Massahi, Desiree D. M. Ferreira, "Thin film coating and characterisation of the BEaTriX mirrors," DTU technical report BEaTriX/0001(1), 1 Dec 2020

Reference documents

[RD1]. B. Salmaso, S. Basso, E. Giro, D. Spiga, G. Sironi, et al., "BEaTriX - the Beam Expander Testing X-Ray facility for testing ATHENA's SPO modules: progress in the realization," Proc. SPIE 11119, 111190N (2019)

[RD2]. Salmaso, B., Spiga, D., "The BEaTriX parabolic mirror: manufacturing tolerances and expected results in UV and X-ray illumination," INAF/OAB technical report 05/2018

[RD3]. Stover, J. C., "Optical scattering: measurement and analysis," SPIE Optical Engineering Press (1995)

[RD4]. Raimondi, L., Spiga, D., "Mirrors for X-ray telescopes: Fresnel diffraction-based computation of point spread functions from metrology," Astronomy & Astrophysics, Volume 573, id. A22 (2015)

Acronyms

ATHENA Advanced Telescope for High-Energy Astrophysics
BEaTriX   Beam Expander Testing X-ray facility
DTU   Denmark Technical University
EA   Effective Area
ESA   European Space Agency
HEW   Half Energy Width
INAF   Istituto Nazionale di Astrofisica
OAB   Osservatorio Astronomico di Brera
PSD   Power Spectral Density
PSF   Point Spread Function
XRR   X-ray Reflectivity
XRS   X-ray Scattering

1. Scope of the document

This brief document reports the characterizations of X-ray reflectivity and scattering performed on platinum coating samples deposited at DTU on superpolished (σ < 2 Å) fused silica substrates. The samples represent preliminary tests for the deposition of the reflective coating on the parabolic mirror (in HOQ310 fused quartz) of the BEaTriX X-ray facility, in construction at INAF-OAB [RD1, RD2]. The X-ray characterizations that have been performed at INAF-OAB encompass XRR tests at 8.045 keV, and low-res XRS measurements at the same energy. While the former returns a single roughness rms value within a non-precisely identified spatial frequency range, the latter return a reliable method for an independent measurement of the surface PSD.

2. Setup description

The substrates have been procured and characterized in XRR-XRS by INAF-OAB and coated at DTU Space with thin (30 nm) layers of platinum using the dedicated sputtering facility. Prior to deposition, the reflectivity of the substrates was measured at 1.5 keV, inferring an equivalent σ of about 2 Å. One sample (G1) was subsequently coated with a simple platinum layer, while G2 and G3 had a thin chromium layer (4 nm) deposited on glass before the Pt deposition. After coating, the XRR reflectivity of the samples [AD1] was tested at 8.045 keV before being shipped to INAF-OAB. The Cr layer was used to enhance the adhesion of the Pt layer on the glass surface.
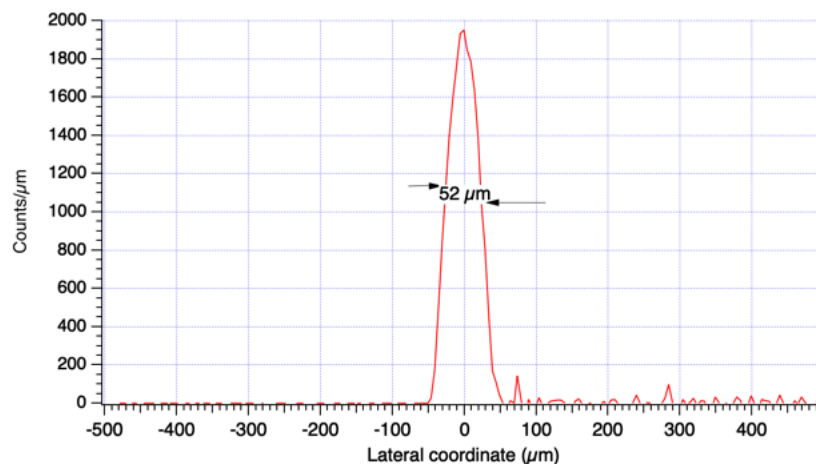

Figure 1: measured width of the beam obtained in the X-ray setup adopted at INAF-OAB. The profile is obtained from a knife-edge scan using the G1 sample itself, after a careful alignment to the oncoming beam.

The BEDE-D1 diffractometer, working at 8.045 keV, has been equipped with a double monochromator and a 100 µm-slit at the monochromation stage exit, plus a 50 µm slit near the sample to make the beam narrow in the horizontal plane direction. Owing to the small size of samples (1 inch), this allows us collecting all the incident beam even at low grazing angles. The beam has been characterized by a knife-edge scan, which, by differentiation, returns the beam intensity profile (Figure 1). The beam width is just 52 µm, enabling full XRS measurements at angles larger than 630 arcsec. The measurement results are shown in the next sections.

3. X-Ray measurements
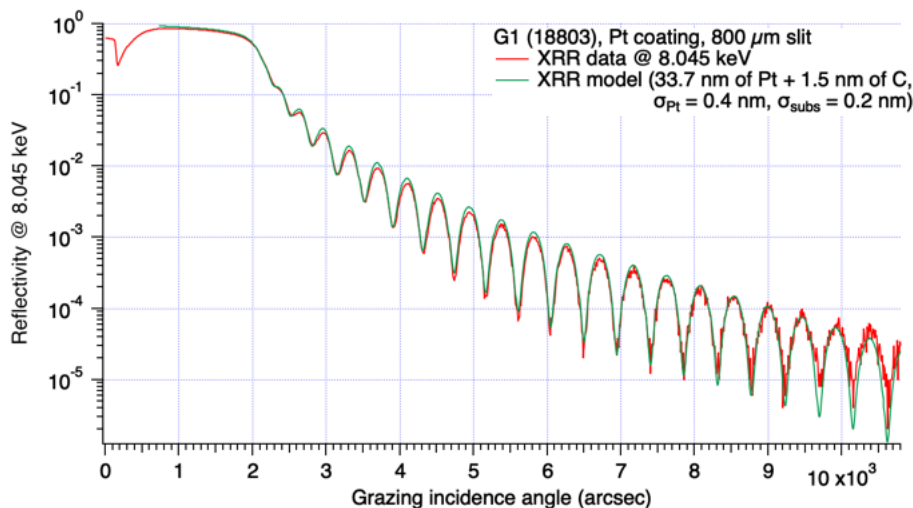
3.1.   XRR measurements at 8.045 keV

Figure 2: XRR measurement at 8.045 keV of the sample G1, with simple platinum coating. A thin layer of C contaminations had to be assumed, as suggested in the DTU report [AD1], in order to match the model to the experimental data at low incidence angles.

The XRR scan of the G1 sample (only platinum), collected with an 800 µm-wide slit on the scintillator detector, at a distance of approximately 400 mm from the sample, is shown in Figure 2. Clear interference fringes are observed beyond the critical angle of platinum. By fitting a simple reflectance model, we obtain that the platinum layer has a 33.7 nm thickness and a density very close to the nominal one. As already noticed by DTU, data are compatible with a molecular layer of hydrocarbons (1.5 nm), which we have modeled as a thin layer of amorphous carbon. As for the roughness, while the fused silica substrate fits with a 2 Å rms value (as expected), the platinum-air interface has a roughness close to 4 Å. Counting the angular acceptance of the detector, one can estimate that this value should refer to all spatial frequencies > (4 µm)$^{-1}$.
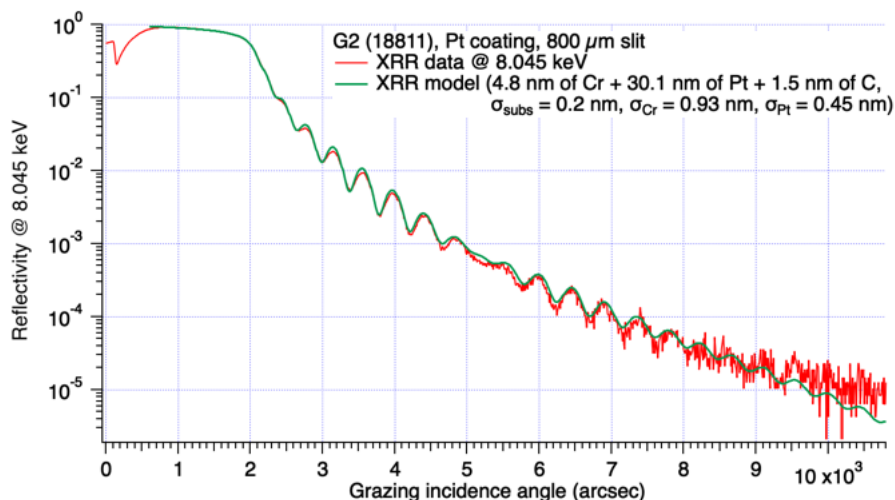

Figure 3: XRR measurement at 8.045 keV of the sample G2, with chromium and platinum layers. In this case also, a thin layer of C contaminant was needed to improve the model-to-data matching at low incidence angles. The platinum roughness is not significantly higher than the previous sample, it is the lower (Cr-Pt) interface that is rougher or interdiffused (that does not harm the reflectivity in the BEaTriX mirror operation).
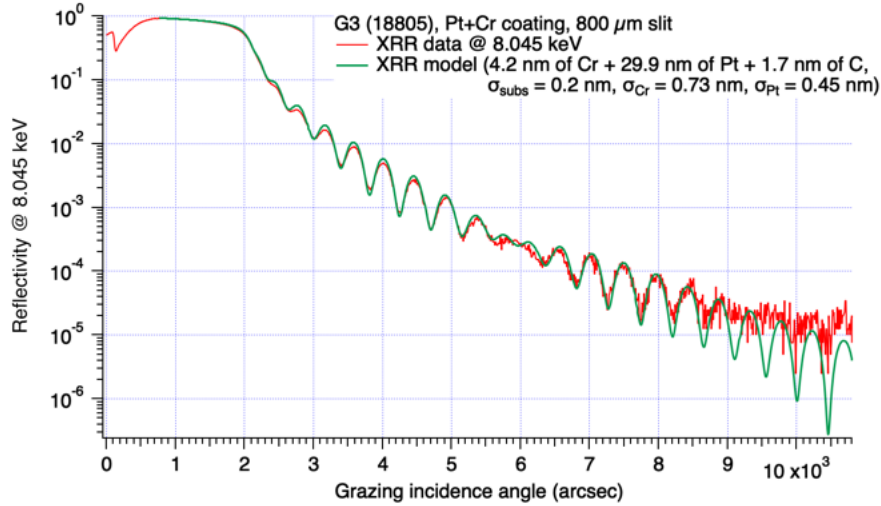
Figure 4: XRR measurement at 8.045 keV of the sample G3, with chromium and platinum layers. In this case also, a thin layer of C contaminant was needed to improve the model-to-data matching at low incidence angles. The platinum roughness is not significantly higher than the previous sample, it is the lower (Cr-Pt) interface that is rougher or interdiffused (that does not harm the reflectivity in the BEaTriX mirror operation).

Figure 3 and Figure 4, in contrast, display the XRR scans obtained with exactly the same setup as for G1, of the two samples with chromium interlayer. Fringes appear clearly, albeit less pronounced as a result of a triple interface interference. In practice, there are two system of fringes that interfere with each other, causing the central "node" in the vicinities of 5000 - 6000 arcsec. The platinum layer is, this time, slightly thinner and closer to the nominal value (30 nm), while the chromium layer is 4-5 nm thick. It is important to note that the roughness of the outer platinum surface (4.5 Å) as inferred from the XRR scan is only slightly rougher than that on sole platinum. Unlike the outermost interface, the chromium-platinum interface exhibits high roughness (which agrees with the conclusions of DTU [AD1]), or, more likely, high interdiffusion. This "fuzzy" interface has no impact on the reflectivity at incidence angles below the critical one, where the BEaTriX mirror is to be operated.

3.2. Low-res XRS measurements

X-ray scattering measurements, i.e., the angular distribution of rays around the specular reflection, is an important tool aimed at an independent computation of the surface PSD of the roughness. The "low-res" phrase refers to the scanning technique, that is just based on steering the detector around the sample, as opposite to the "high-res" technique based on the rotation of an analyzing crystal. For this analysis, the sole low-res technique was used. A summary of all the scattering measurements is displayed in Figure 5.

The XRS uncoated substrates were measured prior to deposition at a different angle (cyan line, re-aligned). The other coatings scatter the beam depending on their roughness PSD, and, as expected, more than uncoated fused silica. Also shown is the Pt reflectivity, used in scattering data reduction and responsible for the "bump" in the green line. The formula relating the PSD to the scattering distribution is (see. e.g., [RD3]):

$$\frac{1}{I_0}\frac{dI_S}{d\vartheta_s} = \frac{16\pi^2}{\lambda^3}\sin\vartheta_i\sin^2\vartheta_s\sqrt{R(\vartheta_i)R(\vartheta_s)}\,PSD(l) \qquad (1)$$

where $\theta_i = 0.3$ deg is the incidence angle, θ_s the scattering angle (both measured from the surface), R is the nominal reflectivity of platinum at the angle θ and the X-ray wavelength λ, and l is the spatial wavelength:

$$l = \frac{\lambda}{\cos\vartheta_i - \cos\vartheta_s} \qquad (2)$$

which is, basically, the grating equation applied at the 1-st diffraction order. Figure 5 also shows that the bare platinum layer (green line) scatters more than the one with chromium interlayer (blue and purple lines), even they were taken at the same energy and the same incidence angle. This suggest higher roughness of the G1 sample, which is easily confirmed by a visual inspection of samples under an intense light beam (see cover images), but the spatial frequencies involved in roughening are low enough to be missed in the XRR scan, as they scatter at angles within the slit on the detector (Sect. 3.1). Applying Eqs. 1 and 2 to XRS data, we easily obtain the PSDs in Figure 6. G1 (Pt only) is certainly rougher, which confirms the visual inspection.
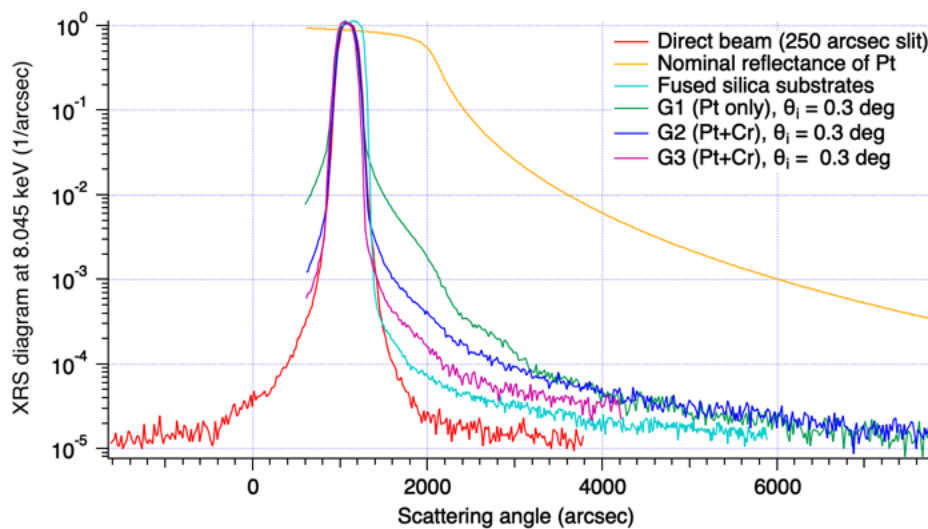

Figure 5: X-ray scattering diagrams for the three coated samples in low-resolution mode, at the incidence angle of 0.3 deg off-surface. The diagrams were normalized to the incident beam. Scattering is apparent from the excess of counts on the right side of the direct beam scan (red line).
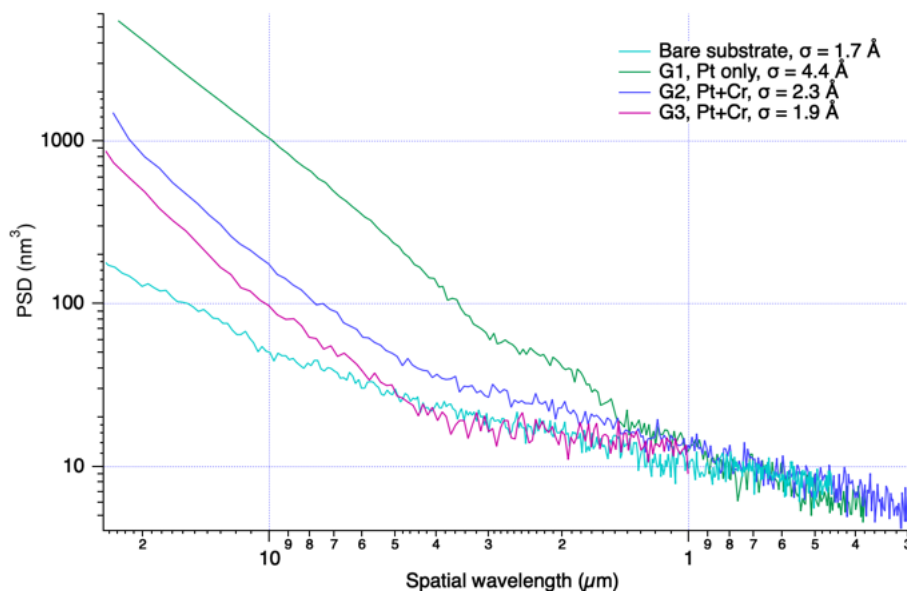

Figure 6: the PSD computed from the low-resolution scattering data shown in Figure 5. the substrate has nearly the same PSD as the coated samples at high frequency, even if it scatters much less, because the glass reflectivity at these scattering angles is much lower than that of platinum (see the effect of reflectivity in Eq.1).

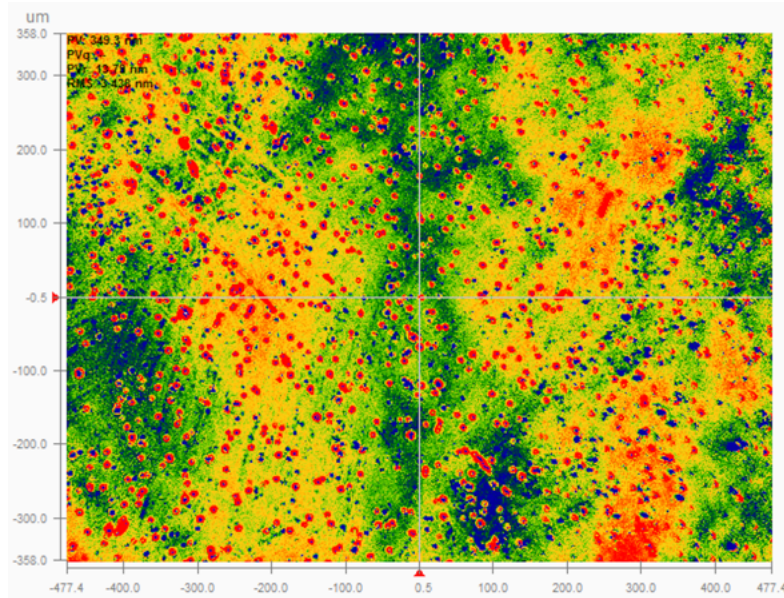# 4. Direct topography measurements

Figure 7: MFT 10x image sampled on G1 (platinum on fused silica). The surface appears covered with point-like defects in relief.

In order to have an independent confirmation of the different behavior observed in the samples characterized in X-rays in the previous section, we have directly inspected the topography of the same samples via MFT 10× (MicroFinish Topography) operated at OAB. A representative image of the G1 sample is shown in Figure 7. The platinum surface appears covered with point-like defects, mostly in relief, superposed to the glass substrate topography. Such defects are not visible (or very rarely encountered) in the G2 and G3 samples (Figure 8 and Figure 9), probably due to the enhanced adhesion of platinum to the glass surface via the chromium layer.
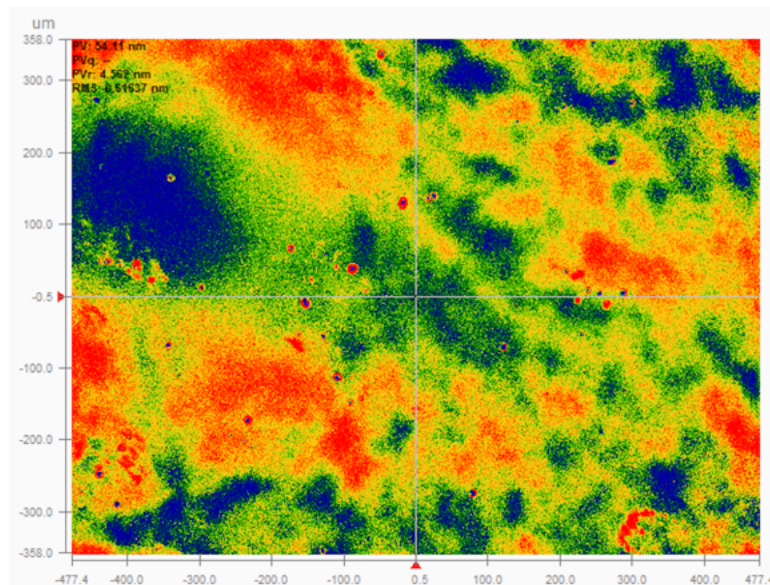

Figure 8: MFT 10x image sampled on G2 (platinum over chromium). The topography does not exhibit the defects seen on G1.
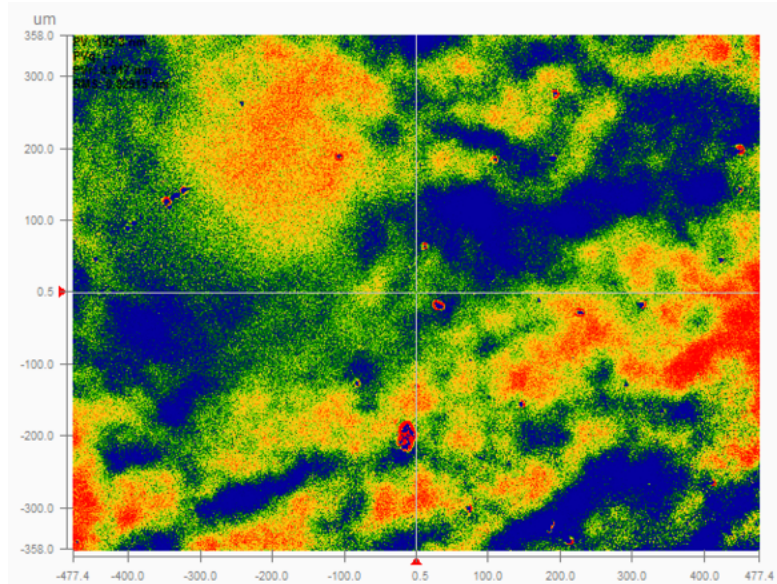
Figure 9: MFT 10x image sampled on G3 (platinum over chromium). Just like G2, the topography appears clear from the defects spread over G1.
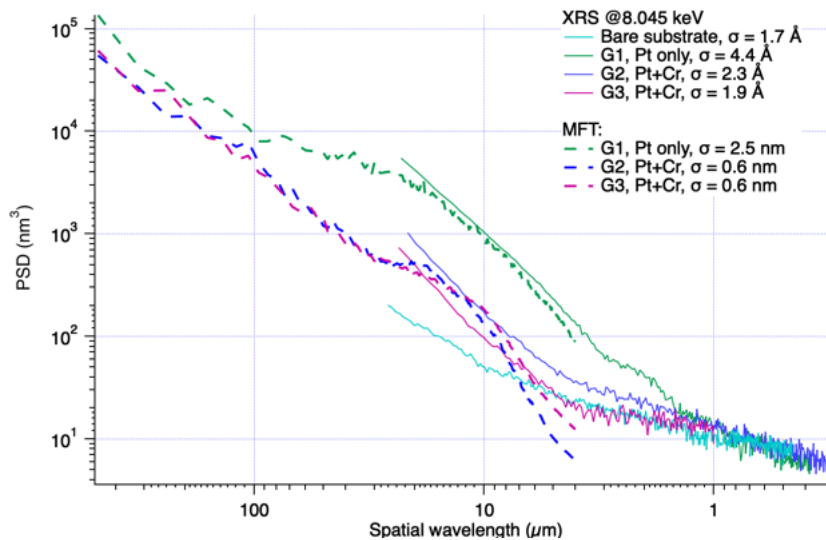

Figure 10: the PSD computed from MFT data, in very good agreement with data from low-res scattering measurement.

The PSDs computed from the measurements are plotted in Figure 10, and in good agreement with the PSD inferred from XRS measurements. It is confirmed that the roughening/aging of the platinum layer on glass exceeds the one of Pt+Cr, chiefly in the 100 – 2 µm range of spectral periods. As the topography at spatial scales longer than 100 µm is dominated by the glass substrate relief, the PSDs at spatial periods greater than 100 µm tend to merge.

5. Conclusions

The measurements performed on the samples coated at DTU suggest that applying a thin layer of chromium before the platinum deposition is beneficial in terms of layer adhesion and stability and does not seem to significantly degrade the reflectivity. Moreover, it helps reducing surface defects in a relevant set of spatial

wavelengths (100 – 2 μm), as it could be detected with both XRS and MFT measurements. A comparison of the PSDs along with the current spec for the BEaTriX mirror is shown in Figure 11. The picture also shows that the roughness growth in Cr-Pt samples is within the tolerance and compatible with the best polishing level attained on the BEaTriX mirror. A high-res diffraction [RD4] computation at 4.51 keV (the highest energy of operation for BEaTriX) shows that a relevant difference in diffuse scattering can be likely expected from the two PSDs (Figure 12), which is once more in favor of the chromium-platinum solution.
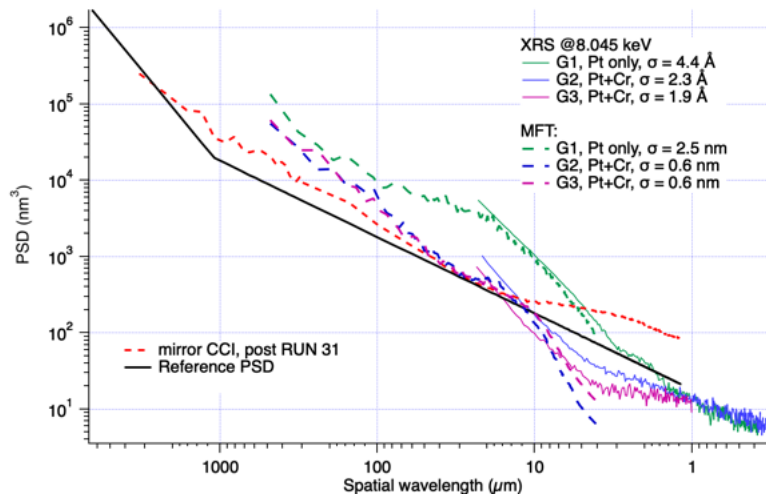

Figure 11: the measured PSDs on the coated samples, in comparison with the refence PSD for the BEaTriX mirror (black-solid line) and the state of the art of the uncoated mirror being polished (red-dashed line).
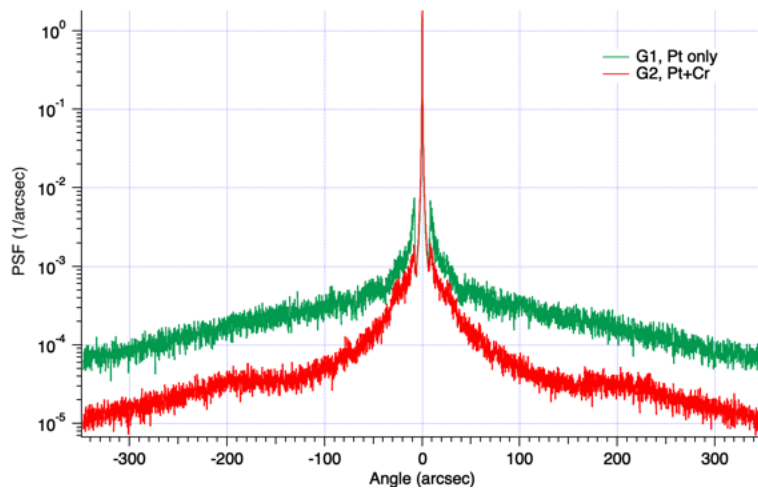

Figure 12: predicted scattering diagram at 4.51 keV from the complete PSD of the samples G1 and G2 (the behavior of G3 is expectedly similar to G2), computed via Fresnel diffraction [RD4]. The HEW of the two diagrams is below 1 arcsec, but the W90 takes on completely different values (150 arcsec for G1, 3 arcsec for G2), as a result of the entirely different wings of the PSF in the two cases.